Analytical first and second energy derivatives of the generalized conductorlike screening model for free energy of solvation

Thanh N. Truong[a] and Eugene V. Stefanovich[b]
Department of Chemistry, University of Utah, Salt Lake City, Utah 84112

(Received 24 March 1995; accepted 25 May 1995)

We present analytical expressions for the first and second energy derivatives of our recently proposed generalized conductorlike screening model (GCOSMO) for free energy of solvation of solute in an arbitrary shape cavity. An application to study hydration effects on structure and stability of glycine zwitterion in aqueous solution is also presented. These calculations were carried out at the Hartree–Fock, second-order Møller–Plesset perturbation theory and different nonlocal density functional theory levels using the 6-31G(d,p) basis set. We found that our quantum mechanical GCOSMO solvation model costs from 10% to 40% extra cpu time per one Berny optimization step compared to the gas-phase calculations for different levels of theory. For the glycine system, the optimized zwitterionic structure in aqueous solution agrees very well with experimental crystal structure and the enthalpy change for transfering glycine from the gas phase to the aqueous solution is also in excellent agreement with experimental data. The ''single point'' approach, which has been used in the past, yields erroneous results. The efficiency and accuracy of our GCOSMO solvation model indicate that this model can be a practical tool for studying structure and activity of moderately large biological systems in solutions. © *1995 American Institute of Physics.*

I. INTRODUCTION

The availability of analytical energy derivatives for an accurate *ab initio* quantum mechanical solvation model would greatly enhance the efficiency and accuracy of molecular modeling of solvent effects on structures and conformational equilibria, more importantly, it opens the possibility for quantitatively studying potential energy surfaces, chemical reactions and spectroscopic properties of solvated systems. In order to adequately model chemical reactions in solutions, the quantum mechanical description of the solute electrons must be sufficiently accurate. In this case, the semiempirical molecular orbital approach is less appropriate, though it has been used successfully in modeling solvation energy of equilibrium structures. We limit our discussion only to solvation models within *ab initio* molecular orbital or density functional theory frameworks and refer readers to the two recent reviews[1,2] for more detailed discussion with complete references in the semiempirical and classical approaches. In particular, we focus on the development and implementation of analytical energy derivatives of dielectric continuum solvation models.

In the dielectric continuum approach, solvated system is modeled as the solute inside a cavity surrounded by a dielectric continuum medium with the dielectric constant ϵ. For solute in an arbitrary shape cavity, the polarizable continuum model[3,4] (PCM), combined density functional theory (DFT) PCM[5] or with classical Poisson–Boltzmann electrostatic solvation model[6–8] (DFT/PB), and our recently proposed generalized conductorlike screening model[9–11] (GCOSMO) have shown to be promising for calculating accurate free energy of solvation. Analytical first and second energy derivatives for the PCM model within the Hartree–Fock (HF) formalism have been derived.[12,13] However, the expressions of these derivatives are complicated and practical applications have not been done. Electrostatic gradients of the classical PB method have been proposed[14] but have not been used in the DFT/PB approach. To date, gas-phase geometries have been used to calculate solvation energies in most studies using the PCM and DFT/PB methods, though nongradient optimization procedures had been previously proposed.[15]

The GCOSMO solvation model[9] recently proposed by us can be incorporated straightforwardly into classical, *ab initio* molecular orbital and density functional theory frameworks. This model is a generalization of the semiempirical COSMO model.[16] The original COSMO model[16] only calculates electrostatic solvation free energy by representing the solute as a set of point charges and dipoles in the neglect differential diatomic overlap formalism, whereas our GCOSMO model not only has a general description for the solute charge density but also includes dispersion, repulsion, and cavity formation contributions.[11] An advantage of our quantum GCOSMO solvation model is that the solvent effects are included directly in the Hartree–Fock–Roothan formalism as additional terms to the Fock matrix elements.[9] As results, the cpu time required for a single point calculation using our model is only on the average of 10% longer than the gas-phase calculation while it is several times to an order of magnitude longer for the DFT/PB approach and iterative formulation of the PCM method due to the coupled iterative procedures. Recent matrix and partial closure formulations[17] of the PCM method converge the surface charges and the solute electron density simultaneously in the same SCF step, thus are expected to have comparable performance with our GCOSMO model. We have performed studies on the convergency, accuracy and validity of GCOSMO for calculating

[a]Author to whom all correspondence should be addressed.
[b]On leave from the Institute of Chemical Physics, University of Latvia, 19 Rainis Blvd., Riga LV1586, Latvia.

hydration energies of neutral and ionic molecules as well as reaction profile of an S_{N^2} reaction in aqueous solution and reported in separate papers.[9–11] These studies showed that GCOSMO is an efficient and accurate tool for modeling chemical phenomena in solvents with high dielectric constants.

It should be noted that alternatively, solvent–solute interactions can be modeled explicitly by including a small number of nearest neighbor solvent molecules in the full quantum calculations as in the supermolecule approach.[18] This approach has been employed to study structures and reactivities of small hydrated clusters.[18,19] The large number of soft vibrational modes, however, makes the geometry optimization for global minimum very difficult. Furthermore, this approach, cannot include the effect of the long-range electrostatic interaction with the bulk solvent. Recent combined quantum mechanics/molecular mechanics approaches[20–24] with available energy gradients can account the solute electron redistribution. The proposed frozen density approach[25] gives a more accurate description for solvent, though analytical energy gradients are not yet available. These new approaches offer promising alternatives for classical molecular dynamics or Monte Carlo simulations of reactions in solution, though computational demand would be quite substantial. Also, detailed analysis on the accuracy of these methods for modeling solvent effects on solute structures has not yet been done and it is certainly needed.

In this study, we present analytical expressions for the first and second energy derivatives with respect to the solute nuclear coordinates for our GCOSMO dielectric continuum solvation model. Comparing to those of the PCM model, the GCOSMO derivatives have much simpler expressions. We have implemented the GCOSMO energy gradients into the HF, DFT, and second-order Møller–Plesset perturbation levels of theory. To illustrate the efficiency of the GCOSMO energy gradients, we have applied them to study hydration effects on structures and relative stabilities of neutral and zwitterionic forms of glycine. To our knowledge, this is the first *ab initio* dielectric continuum solvation study where solute in an arbitrary shape cavity is fully optimized using gradient technique.

Glycine being the simplest amino acid has been the focus of many theoretical studies[26–38] both in the gas phase and in solution. Most theoretical studies, however, have been focused on the conformations of glycine in the gas phase,[29–33,36,37,39,40] only a few qualitative studies[26–28,33–35,41] exist on the hydration effects on their structures and relative stability. It has been known that glycine only exists in the neutral form (NT) in the gas phase, but in aqueous solution or solid, its zwitterionic form (ZT) is more stable and predominant. The experimental estimates for the enthalpy[42] of transferring glycine from the gas phase to aqueous solution and the free energy difference[43] between the neutral and zwitterion forms of glycine in aqueous solution as well as crystal structure[44] of glycine zwitterion are available. Such information can be used to test the accuracy of our method. In Sec. II, we derive the expressions for the first and second derivatives of GCOSMO which can be incorporated into HF, DFT, and MP2 levels of theory. We discuss the results for glycine in both gas phase and aqueous solution as well as the accuracy and efficiency of GCOSMO in Sec. III. The conclusion is given in Sec. IV.

II. GENERALIZED CONDUCTORLIKE SCREENING MODEL (GCOSMO)

The essence of both COSMO and GCOSMO methods is first to determine the surface charges $\sigma(\mathbf{r})$ on the surface (S) of the cavity for a screening conductor (the dielectric constant $\epsilon=\infty$) from a boundary condition that the electrostatic potential on the surface S is zero,

$$\sum_i \frac{z_i}{|\mathbf{r}-\mathbf{R}_i|} - \int_V \frac{\rho(\mathbf{r}')}{|\mathbf{r}-\mathbf{r}'|}\, d^3r' + \int_S \frac{\sigma(\mathbf{r}')}{|\mathbf{r}-\mathbf{r}'|}\, d^2r' = 0, \tag{1}$$

where $\mathbf{r}$ is on S; ρ is the solute electron density; z_i and $\mathbf{R}_i$ are the nuclear charge and position vector of atom i. For a dielectric medium specified by the dielectric constant ϵ, the surface charges are then determined approximately in GCOSMO by scaling the screening conductor surface charge by a factor of $f(\epsilon)=(\epsilon-1)/\epsilon$ to satisfy the Gauss theorem for the total surface charge. An empirical scaling factor of $(\epsilon-1)/(\epsilon+\frac{1}{2})$ was used in COSMO.[16]

For a cavity boundary defined by M surface elements with areas $\{S_u\}$ and surface charge density at each surface element approximated as a point charge, $\{q_u\}$, located at the center of that element, $\{\mathbf{t}_u\}$, from the above boundary condition the surface charge distribution is given by

$$\mathbf{q} = -f(\epsilon)\mathbf{A}^{-1}(\mathbf{Bz}+\mathbf{c}), \tag{2}$$

where $\mathbf{A}$, $\mathbf{B}$, and $\mathbf{c}$ are $M\times M$, $M\times N$, and $M\times 1$ matrices, respectively, with matrix elements defined by

$$A_{uv} = \frac{1}{|\mathbf{t}_u-\mathbf{t}_v|} \quad \text{for } u\neq v, \text{ and } A_{uu} = 1.07\sqrt{\frac{4\pi}{S_u}}, \tag{3}$$

$$B_{ui} = \frac{1}{|\mathbf{t}_u-\mathbf{R}_i|}, \tag{4}$$

$$c_u = -\int \frac{\rho(\mathbf{r})}{|\mathbf{r}-\mathbf{t}_u|}\, d^3r, \tag{5}$$

and $\mathbf{z}$ is the vector of N nuclear charges. Alternatively, these surface charges can be determined by variationally minimizing the total electrostatic solvation energy

$$\Delta G_{\text{els}}(\mathbf{q}) = \mathbf{z}^\dagger\mathbf{B}^\dagger\mathbf{q} + \mathbf{c}^\dagger\mathbf{q} + \frac{1}{2\, f(\epsilon)}\, \mathbf{q}^\dagger\mathbf{A}\mathbf{q} \tag{6}$$

with respect to $\mathbf{q}$ ($\dagger$ denotes matrix transposition).

Of course, use of a scaling factor to determine the solvent reaction field in GCOSMO is not as rigorous and accurate as boundary condition employed in the PCM formulation. However, we would like to make three remarks in this respect. First, practical implementations of the PCM model also utilize a scaling function,[3,4] however, its primary purpose is to account for numerical errors in the calculation of surface charges. The scaling function $f(\epsilon)$ used in the GCOSMO model is theoretically motivated. Second, as mentioned by Klamt and Schüürmann,[16] the charge scaling introduces a relative error of about ϵ^{-1}, what is less than 1 kcal/

mol for hydration energies of most solutes. Third, the representation of the solvent as a dielectric continuum is a basic approximation for both PCM and GCOSMO models. Thus, validity and accuracy of both approaches depend mainly on the careful selection of fitting parameters—atomic radii. Our studies showed that fitting of atomic radii for GCOSMO allows us to reach acceptable agreement (1–2 kcal/mol) with experimental hydration energies.

A. Energy

By expanding $\mathbf{c}_u$ given by Eq. (5) in a basis set, we obtain

$$c_u = -\left\langle \Psi_0^{\mathrm{HF}} \left| \frac{1}{|\mathbf{r}-\mathbf{t}_u|} \right| \Psi_0^{\mathrm{HF}} \right\rangle = \sum_{\mu\nu} P_{\mu\nu} L^u_{\mu\nu}, \tag{7}$$

where

$$L^u_{\mu\nu} = -\left\langle \mu \left| \frac{1}{|\mathbf{r}-\mathbf{t}_u|} \right| \nu \right\rangle, \tag{8}$$

and $P_{\mu\nu}$ is the density matrix element. The total free energy of the whole system (solute+surface charges) is then given by

$$E_{\mathrm{tot}} = \sum_{\mu\nu} P_{\mu\nu}\left(H_{\mu\nu} + \frac{1}{2} G_{\mu\nu} \right) - \frac{1}{2} f(\epsilon)\mathbf{z}^{+}\mathbf{B}^{+}\mathbf{A}^{-1}\mathbf{B}\mathbf{z} + E_{\mathrm{nn}} + E_{\text{non-els}}, \tag{9}$$

where E_{nn} is the solute nuclear–nuclear repulsion. The solvent contributions to the one and two electron terms of the Fock matrix ($H_{\mu\nu}$ and $G_{\mu\nu}$, respectively) are expressed as

$$H^s_{\mu\nu} = -f(\epsilon)\mathbf{z}^{\dagger}\mathbf{B}^{\dagger}\mathbf{A}^{-1}\mathbf{L}_{\mu\nu}, \tag{10}$$

$$G^s_{\mu\nu} = -f(\epsilon)\mathbf{c}^{\dagger}\mathbf{A}^{-1}\mathbf{L}_{\mu\nu}. \tag{11}$$

$E_{\text{non-els}}$ is the nonelectrostatic part of the free energy of solvation that includes the dispersion, repulsion, and cavity formation contributions.

It is important to point out that in contrast to the current implementations of the PCM method,[17] namely the iterative, closure, and matrix-inversion procedures, where the solvent reaction field is explicitly calculated from the surface charges, our GCOSMO method includes the effects of the solvent reaction field directly in the Fock matrix and thus explicit calculation of surface charges is not needed. This is suitable for implementation of the energy derivatives. Such direct solvent reaction field approach within the PCM formalism has been proposed by Hoshi *et al.*[45–47]

The above formalism is directly applicable for the HF and DFT theories. However, it can be also implemented in the MP2 level of theory by recognizing the following. The effect of the solute electron correlation on the surface charges is accounted in the calculation of vector $\mathbf{c}$. At the MP2 level, it is given by

$$c_u = -\left\langle \Psi_0^{\mathrm{HF}} + \Psi_0^{(1)} \left| \frac{1}{|\mathbf{r}-\mathbf{t}_u|} \right| \Psi_0^{\mathrm{HF}} + \Psi_0^{(1)} \right\rangle \tag{12a}$$

$$= -\left\langle \Psi_0^{\mathrm{HF}} \left| \frac{1}{|\mathbf{r}-\mathbf{t}_u|} \right| \Psi_0^{\mathrm{HF}} \right\rangle - 2\left\langle \Psi_0^{\mathrm{HF}} \left| \frac{1}{|\mathbf{r}-\mathbf{t}_u|} \right| \Psi_0^{(1)} \right\rangle - \left\langle \Psi_0^{(1)} \left| \frac{1}{|\mathbf{r}-\mathbf{t}_u|} \right| \Psi_0^{(1)} \right\rangle \tag{12b}$$

$$= -\left\langle \Psi_0^{\mathrm{HF}} \left| \frac{1}{|\mathbf{r}-\mathbf{t}_u|} \right| \Psi_0^{\mathrm{HF}} \right\rangle - \left\langle \Psi_0^{(1)} \left| \frac{1}{|\mathbf{r}-\mathbf{t}_u|} \right| \Psi_0^{(1)} \right\rangle, \tag{12c}$$

where Ψ_0^{HF} and $\Psi_0^{(1)}$ are the HF ground state wave function and its first order correction in the solvated system. The second term in Eq. (12b) is zero due to the fact that $\Psi_0^{(1)}$ depends only on doubly excited state wave functions and thus will not mix with the reference ground-state wave function in one-electron integrals. Consequently, the first order correction to the wave function, $\Psi_0^{(1)}$, has a second order effect on c_u and thus is expected to be small. In the present study, this contribution is neglected. Thus, the MP2 total energy for solvated system is approximated by adding to the HF energy given in Eq. (9) the second order energy correction, $E^{(2)}$, which depends only on the HF molecular orbitals and orbital energies of the solvated system. Note that our treatment of electron correlation here is equivalent to the perturbation theory at the energy level (PTE) approach proposed for the PCM model by Olivares del Valle and Tomasi.[48] Recent studies[49–52] has shown that, in fact, the PTE term has the largest contribution in the total correlation energy for small neutral solutes. However, the effect of neglecting the second-order term in Eq. (12c) in the calculation of the total derivatives is not known, and thus requires further study.

B. Analytical first derivatives

In this study, we only present the electrostatic contribution to the total derivatives using approach suggested in Ref. 16. Contributions to the total derivatives from the dispersion, repulsion, and cavity formation energies may be important for neutral nonpolar systems and will be considered in a future study. We can rewrite the electrostatic energy of the solvated system in Eq. (9) as

$$E = \sum_{\mu\nu} P_{\mu\nu}\left(H^0_{\mu\nu} + \frac{1}{2} G^0_{\mu\nu} \right) + E_{\mathrm{nn}} + \Delta G_{\mathrm{els}}, \tag{13}$$

where $H^0_{\mu\nu}$ and $G^0_{\mu\nu}$ are the solute one and two electron components of the Fock matrix and involve only the solute electron–electron and electron–nuclei interactions, and ΔG_{els} is given by Eq. (6). The derivative of the total energy in Eq. (13) with respect to the nuclear coordinates $\mathbf{R}_i$ of atom i is given by

$$\boldsymbol{\nabla}_{\mathbf{R}_i}(E) = \boldsymbol{\nabla}_{\mathbf{R}_i}(E^*) + \boldsymbol{\nabla}^*_{\mathbf{R}_i}(\Delta G_{\mathrm{els}}), \tag{14}$$

where $\boldsymbol{\nabla}_{\mathbf{R}_i}(E^*)$ is the derivative of the first two energy terms in Eq. (13) plus the contribution from the partial derivative of the density matrix in the ΔG_{els} term. $\boldsymbol{\nabla}_{\mathbf{R}_i}(E^*)$ has expression similar to that of the HF theory for a system *in vacuo*,[53]

$$\nabla_{\mathbf{R}_i}(E^*)=\sum_{\mu\nu} P_{\mu\nu}\nabla_{\mathbf{R}_i}(H^0_{\mu\nu}) + \frac{1}{2}\sum_{\substack{\mu\nu\\ \lambda\sigma}} P_{\mu\nu}P_{\lambda\sigma}\nabla_{\mathbf{R}_i}(\mu\lambda\|\nu\sigma)+\nabla_{\mathbf{R}_i}(E_{\rm nn}) - \sum_{\mu\nu} W_{\mu\nu}\nabla_{\mathbf{R}_i}(S_{\mu\nu}), \tag{15}$$

where $W_{\mu\nu}$ is an energy-weighted density matrix containing the solvent effects. The second term in Eq. (14) is due to the electrostatic solvation energy and is given by

$$\nabla^*_{\mathbf{R}_i}(\Delta G_{\rm els})=\mathbf{z}^\dagger(\nabla_{\mathbf{R}_i}\mathbf{B}^\dagger)\mathbf{q}+(\nabla^*_{\mathbf{R}_i}\mathbf{c}^\dagger)\mathbf{q}+\frac{1}{2f}\mathbf{q}^\dagger(\nabla_{\mathbf{R}_i}\mathbf{A})\mathbf{q} + \left\{\mathbf{z}^\dagger\mathbf{B}^\dagger+\mathbf{c}^\dagger+\frac{1}{f}\mathbf{q}^\dagger\mathbf{A}\right\}\nabla_{\mathbf{R}_i}\mathbf{q}. \tag{16}$$

From Eq. (2), the expression in the curly brackets in Eq. (16) is zero, thus the derivative of the surface charges is not needed. Note that in the PCM model, this derivative is required.[12,13] Equation (16) becomes

$$\nabla^*_{\mathbf{R}_i}(\Delta G_{\rm els})=\mathbf{z}^\dagger(\nabla_{\mathbf{R}_i}\mathbf{B}^\dagger)\mathbf{q}+(\nabla^*_{\mathbf{R}_i}\mathbf{c}^\dagger)\mathbf{q}+\frac{1}{2f}\mathbf{q}^\dagger(\nabla_{\mathbf{R}_i}\mathbf{A})\mathbf{q}. \tag{17}$$

If we assume that atomic radii used to define the cavity are fixed, and surface elements stick to the atom they belong, then

$$\nabla_{\mathbf{R}_i}(A_{uv})=-\frac{(\mathbf{t}_u-\mathbf{t}_v)}{|\mathbf{t}_u-\mathbf{t}_v|^3}[\nabla_{\mathbf{R}_i}(\mathbf{t}_u-\mathbf{t}_v)] =-\frac{(\mathbf{t}_u-\mathbf{t}_v)}{|\mathbf{t}_u-\mathbf{t}_v|^3}(\theta_{ui}-\theta_{vi}), \tag{18}$$

with

$$\theta_{ui}=\begin{cases}0 & \text{for } u\notin \text{sphere of atom } i\\ 1 & \text{for } u\in \text{sphere of atom } i\end{cases}. \tag{19}$$

The derivative of the diagonal elements of $\mathbf{A}$, $\nabla_{\mathbf{R}_i}(\mathbf{A}_{uu})$, depends on $(\partial S_u/\partial\mathbf{R}_i)$, i.e., the change in the surface area of the element u with respect to the change in the position of atom i. Thus, only surface elements at the overlapping regions of the atomic sphere of atom i with the neighbor spheres have nonzero $(\partial S_u/\partial\mathbf{R}_i)$. These regions are well defined if the van der Walls surface is used. In fact, an expression for these terms given in the derivatives of the PCM model can also be used here.[12] However, it is not obvious how to determine these terms analytically when the solvent excluding surface[54] is used, particularly when additional spheres were created in regions that were not represented by the van der Walls spheres. To estimate these terms, we have performed numerical differentiations for several systems and found these components very small. Thus, for all practical purposes, it is reasonable to assume that (see also Ref. 16)

$$\nabla_{\mathbf{R}_i}(A_{uu})=0, \tag{20}$$

though, further analysis on the accuracy of this approximation is certainly needed. Finally, differentiating B_{uj} and c_u in Eqs. (4) and (7), we obtain

$$\nabla_{\mathbf{R}_i}(B_{uj})=-\frac{(\mathbf{t}_u-\mathbf{R}_j)}{|\mathbf{t}_u-\mathbf{R}_j|^3}[\nabla_{\mathbf{R}_i}(\mathbf{t}_u-\mathbf{R}_j)] =-\frac{(\mathbf{t}_u-\mathbf{R}_j)}{|\mathbf{t}_u-\mathbf{R}_j|^3}(\theta_{ui}-\delta_{ij}), \tag{21}$$

$$\nabla^*_{\mathbf{R}_i}(c_u)=\sum_{\mu\nu} P_{\mu\nu}\left\langle \mu\left|\frac{(\mathbf{r}-\mathbf{t}_u)}{|\mathbf{r}-\mathbf{t}_u|^3}[-\nabla_{\mathbf{R}_i}(\mathbf{t}_u)]\right|\nu\right\rangle = -\sum_{\mu\nu} P_{\mu\nu}\left\langle \mu\left|\frac{(\mathbf{r}-\mathbf{t}_u)}{|\mathbf{r}-\mathbf{t}_u|^3}\theta_{ui}\right|\nu\right\rangle. \tag{22}$$

"Star" denotes that Eq. (22) is not the complete derivative $\nabla_{\mathbf{R}_i}(c_u)$; the term containing the partial derivative of the density matrix, $P_{\mu\nu}$, was already included in the last term of Eq. (15).

The above energy gradients are valid for the HF and DFT formalisms. However, the same approach can be used for the MP2 energy gradients by adding $\nabla_{\mathbf{R}_i}(\Delta G_{\rm els})$ given in Eq. (17) to the MP2 derivative $\nabla_{\mathbf{R}_i}(E^*)$. We have implemented the GCOSMO energy gradients to the HF, DFT, and MP2 levels of theory by modifying the G92/DFT program.[55]

C. Analytical second derivatives

The second derivative of the total energy with respect to the $\mathbf{R}_i$ and $\mathbf{R}_j$ solute nuclear coordinates can be obtained by differentiating the first derivative given in Eq. (14),

$$\frac{\partial^2 E}{\partial\mathbf{R}_j\partial\mathbf{R}_i}=\frac{\partial^2 E^*}{\partial\mathbf{R}_j\partial\mathbf{R}_i}+\frac{\partial^2{}^*(\Delta G_{\rm els})}{\partial\mathbf{R}_j\partial\mathbf{R}_i}, \tag{23}$$

where the first term has the same form as for the gas phase[53]

$$\frac{\partial^2 E^*}{\partial\mathbf{R}_j\partial\mathbf{R}_i}=\frac{\partial}{\partial\mathbf{R}_j}\left(\frac{\partial E^*}{\partial\mathbf{R}_i}\right) =\sum_{\mu\nu} P_{\mu\nu}\left(\frac{\partial^2 H^0_{\mu\nu}}{\partial\mathbf{R}_j\partial\mathbf{R}_i}\right) + \frac{1}{2}\sum_{\mu\nu\lambda\sigma} P_{\mu\nu}P_{\lambda\sigma}\left(\frac{\partial^2}{\partial\mathbf{R}_j\partial\mathbf{R}_i}\right)(\mu\lambda\|\nu\sigma) + \frac{\partial^2 E_{\rm nn}}{\partial\mathbf{R}_j\partial\mathbf{R}_i}-\sum_{\mu\nu} W_{\mu\nu}\left(\frac{\partial^2 S_{\mu\nu}}{\partial\mathbf{R}_j\partial\mathbf{R}_i}\right)+\sum_{\mu\nu}\left(\frac{\partial P_{\mu\nu}}{\partial\mathbf{R}_j}\right) \times\left(\frac{\partial H^0_{\mu\nu}}{\partial\mathbf{R}_i}\right)+\sum_{\mu\nu\lambda\sigma}\left(\frac{\partial P_{\mu\nu}}{\partial\mathbf{R}_j}\right)P_{\lambda\sigma}\left(\frac{\partial}{\partial\mathbf{R}_i}\right) \times(\mu\lambda\|\nu\sigma)-\sum_{\mu\nu}\left(\frac{\partial W_{\mu\nu}}{\partial\mathbf{R}_j}\right)\left(\frac{\partial S_{\mu\nu}}{\partial\mathbf{R}_i}\right), \tag{24}$$

and

$$\frac{\partial^{2*}(\Delta G_{\rm els})}{\partial \mathbf{R}_j \partial \mathbf{R}_i} = \frac{\partial}{\partial \mathbf{R}_j}\left[\frac{\partial^*(\Delta G_{\rm els})}{\partial \mathbf{R}_i}\right] = \mathbf{z}^\dagger \frac{\partial^2 \mathbf{B}^\dagger}{\partial \mathbf{R}_j \partial \mathbf{R}_i}\,\mathbf{q} + \frac{\partial^{2*}\mathbf{c}^\dagger}{\partial \mathbf{R}_j \partial \mathbf{R}_i}\,\mathbf{q} + \frac{1}{2}\frac{1}{f}\,\mathbf{q}^\dagger \frac{\partial^2 \mathbf{A}}{\partial \mathbf{R}_j \partial \mathbf{R}_i}\,\mathbf{q}. \quad (25)$$

By denoting $\mathbf{r}=(x,y,z)$, $\mathbf{R}_i=(X_i,Y_i,Z_i)$, and $\mathbf{t}_u=(x_u,y_u,z_u)$, the partial second derivatives of **A**, **B**, and **c** can be expressed as

$$\frac{\partial^2 A_{uv}}{\partial X_i \partial X_j} = \left[3\,\frac{(x_u-x_v)^2}{|\mathbf{t}_u-\mathbf{t}_v|^5} - \frac{1}{|\mathbf{t}_u-\mathbf{t}_v|^3}\right](\theta_{ui}-\theta_{vi}) \times (\theta_{uj}-\theta_{vj}), \quad (26)$$

$$\frac{\partial^2 A_{uv}}{\partial Y_i \partial X_j} = 3\,\frac{(y_u-y_v)(x_u-x_v)}{|\mathbf{t}_u-\mathbf{t}_v|^5}\,(\theta_{ui}-\theta_{vi})(\theta_{uj}-\theta_{vj}), \quad (27)$$

$$\frac{\partial^2 A_{uu}}{\partial X_i \partial X_j} = \frac{\partial^2 A_{uu}}{\partial Y_i \partial X_j} = 0, \quad (28)$$

$$\frac{\partial^2 B_{uk}}{\partial X_i \partial X_j} = \left[3\,\frac{(x_u-X_k)^2}{|\mathbf{t}_u-\mathbf{R}_i|^5} - \frac{1}{|\mathbf{t}_u-\mathbf{R}_i|^3}\right](\theta_{uj}-\delta_{kj}) \times (\theta_{ui}-\delta_{ki}), \quad (29)$$

$$\frac{\partial^2 B_{uk}}{\partial Y_i \partial X_j} = 3\,\frac{(y_u-Y_k)(x_u-X_k)}{|\mathbf{t}_u-\mathbf{R}_i|^5}\,(\theta_{uj}-\delta_{kj})(\theta_{ui}-\delta_{ki}), \quad (30)$$

$$\frac{\partial^{2*} c_u}{\partial X_i \partial X_j} = \frac{\partial}{\partial X_i}\left(\frac{\partial^* c_u}{\partial X_j}\right) = -\sum_{\mu\nu} P_{\mu\nu}\langle\mu\left|3\,\frac{(x-x_u)^2}{|\mathbf{r}-\mathbf{t}_u|^5} - \frac{1}{|\mathbf{r}-\mathbf{t}_u|^3}\right|\theta_{ui}\theta_{uj}|\nu\rangle - \sum_{\mu\nu}\left(\frac{\partial P_{\mu\nu}}{\partial X_i}\right) \times \langle\mu|\frac{(x-x_u)}{|\mathbf{r}-\mathbf{t}_u|^3}\,\theta_{uj}|\nu\rangle, \quad (31)$$

$$\frac{\partial^{2*} c_u}{\partial Y_i \partial X_j} = \frac{\partial}{\partial Y_i}\left(\frac{\partial^* c_u}{\partial X_j}\right) = -\sum_{\mu\nu} P_{\mu\nu}\langle\mu\left|3\,\frac{(x-x_u)(y-y_u)}{|\mathbf{r}-\mathbf{t}_u|^5}\right|\theta_{ui}\theta_{uj}|\nu\rangle - \sum_{\mu\nu}\left(\frac{\partial P_{\mu\nu}}{\partial Y_i}\right)\langle\mu|\frac{(x-x_u)}{|\mathbf{r}-\mathbf{t}_u|^3}\,\theta_{uj}|\nu\rangle. \quad (32)$$

These derivatives are for the HF and DFT formalisms, though they can also be incorporated into the MP2 level of theory for the same reasons as discussed above.

III. RESULTS AND DISCUSSION

In this study, we have tested the accuracy and efficiency of the above analytical first energy derivatives of our GCOSMO solvation model within the *ab initio* molecular orbital (MO) and DFT formalisms by applying them to study hydration effects on structure and stability of glycine in aqueous environment (ϵ=80.0). We have used the solvent excluding surface[54] to define the cavity boundary with the GCOSMO-optimized atomic radii [H: 1.172; O: 1.576; N: 1.738; C(sp^2): 1.635 and C(sp^3): 2.096]. These atomic radii were determined from fitting to experimental free energies of solvation for a set of 12 neutral polar and 5 nonpolar molecules as well as a set of 7 anions and 14 cations at the HF, nonlocal DFT and MP2 levels of theory. The rms differences are about 1 kcal/mol for neutral molecules and 2 kcal/mol for ions. The details on the optimization of atomic radii for our GCOSMO model will be published in a separate report.[56] Dispersion and repulsion contributions were included by using Floris *et al.*'s method[57] with the OPLS parameters.[58] Cavity formation contribution was calculated using the scaled particle theory originally proposed by Pierotti.[59] In all calculations presented below, the 6-31G(d,p) basis set was used. Geometries for both the gas-phase and liquid-phase glycine neutral and zwitterionic forms were fully optimized at the HF, MP2, B3LYP and BH&HLYP levels of theory. B3LYP and BH&HLYP are the nonlocal DFT methods where the hybrid Becke three-parameter[60] (B3) and Becke half and half[61] (BH&H) functional for exchange were used, respectively, in combination with the Lee–Yang–Parr[62] (LYP) functional for correlation. Note that for the neutral form (NT), we used the experimentally determined most stable conformation in the gas phase.[63] For the glycine zwitterionic form (ZT), we used the crystal conformation.[44]

A. Hydration effects on the structure and relative stability of glycine zwitterion

The optimized gas-phase geometries for glycine calculated at the B3LYP and BH&HLYP levels are given in Table I along with the previous CCSD results[31] and experimental data.[64] HF and MP2 geometries have been reported in previous studies,[30,32] thus do not need to be repeated here. Note that both B3LYP and BH&HLYP geometries agree very well with the more accurate *ab initio* CCSD results and with the experimental data with the differences of less than 0.03 Å in the bond lengths and 3° in the angles. B3LYP method yields slightly more accurate geometries. This is in fact consistent with previous studies.[65,66]

The optimized liquid-phase geometries for neutral glycine are given in Table II. We found that aqueous solvent has small effect on the geometry of neutral glycine at all levels of theory. Only small differences with the gas-phase geometries are found in the H–O–C angle. In particular, solvent reaction field opens the H–O–C angle by about 2°. This, however, is within the uncertainty of our GCOSMO model (see below), thus we conclude that aqueous solvent has negligible effect on the structure of the neutral glycine.

The calculated gas-phase and liquid-phase geometries and experimental crystal structure for glycine zwitterion are given in Table III. Although the crystal field is somewhat different from the solvent reaction field, their effects on the solute structure are expected to be similar. It has been known that glycine zwitterion does not exist in the gas phase.[29] The

TABLE I. Geometrical parameters (bond distances are in Å and angles in deg) of neutral glycine (C_s symmetry) in gas phase.

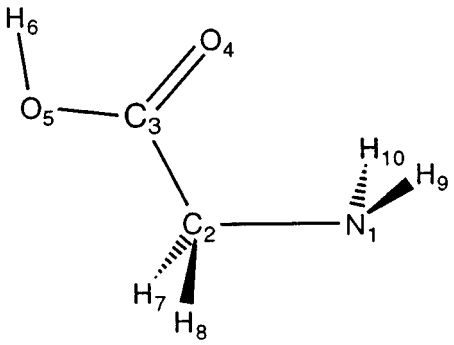

Coordinates	B3LYP	BH&HLYP	CCSD[a]	Expt[b]
N_1–C_2	1.452	1.439	1.458	1.467
C_2–C_3	1.525	1.511	1.525	1.526
C_3–O_4	1.211	1.198	1.216	1.205
C_3–O_5	1.354	1.336	1.359	1.355
O_5–H_6	0.972	0.959	0.972	0.966
C_2–H_7	1.097	1.088	1.098	1.081
N_1–H_9	1.001	1.008	1.021	1.001
N_1–C_2–C_3	115.1	115.0	115.4	112.1
O_4–C_3–C_2	125.2	125.1	125.7	125.1
O_5–C_3–C_2	111.8	111.9	111.5	111.6
H_6–O_5–C_3	106.4	107.3	105.9	
H_7–C_2–N_1	110.0	110.0		
H_9–N_1–C_2	108.9	109.7	108.8	

[a]Were calculated with DZP basis set and are taken from Ref. 31.
[b]Reference 64.

crystal conformation for ZT is, in fact, a local maximum on the gas-phase potential surface. We calculated the gas-phase glycine zwitterionic structure here by fixing C_s symmetry in the experimental conformation only to show the significant magnitude of the hydration effects. Notice that (at the HF level) the C_3–O_5 bond is stretched by 0.025 Å while the C_1–C_3 bond is shortened by 0.038 Å upon hydration. The O_4–C_3–C_1 and N_2–C_1–C_3 angles are noticeably increased by 5–6 as 6°. In other words, the solvent reaction field opens the glycine zwitterionic structure by weakening the electrostatic interaction between the two charged heads. All optimized glycine zwitterionic structures in aqueous solution agree very well with the experimental crystal structure,[44] though BH&HLYP yields slightly better results with the differences of at most 0.009 Å in the bond lengths and 2° in the angles. Thus, our present results are quite encouraging particularly for studying solvent effects on conformations of biological systems.

TABLE II. Geometrical parameters (bond distances are in Å and angles in deg) of neutral glycine (C_s symmetry) in aqueous solution.[a]

Coordinates	HF	MP2	B3LYP	BH&HLYP
N_1–C_2	1.441	1.453	1.455	1.442
C_2–C_3	1.513	1.514	1.523	1.510
C_3–O_4	1.198	1.225	1.218	1.205
C_3–O_5	1.319	1.348	1.347	1.327
O_5–H_6	0.956	0.974	0.974	0.963
C_2–H_7	1.085	1.091	1.097	1.088
N_1–H_9	1.002	1.016	1.020	1.008
N_1–C_2–C_3	115.6	115.3	115.6	115.4
O_4–C_3–C_2	125.4	125.5	125.4	125.2
O_5–C_3–C_2	111.5	111.0	111.4	111.7
H_6–O_5–C_3	110.6	107.8	108.3	108.7
H_7–C_2–N_1	110.1	110.5	109.9	110.1
H_9–N_1–C_2	110.1	108.3	108.7	109.3

[a]Internal coordinates were defined the same as in Table I.

Hydration free energies of neutral and zwitterionic forms of glycine, their relative free energies and enthalpy change ΔH ($NT_{gas} \rightarrow ZT_{solv}$) calculated at the HF, MP2, B3LYP, and BH&HLYP levels are listed in Table IV along with the experimental estimates.[42,43] In order to understand the significance of the present development of analytical derivatives of the GCOSMO solvation model, in Table IV we also give energetic results from ''single point'' calculations, where gas-phase geometries were used for calculations of solvation energies. Note that this is the only available approach for all previous *ab initio* dielectric continuum calculations. Using this ''single point'' approach, we found that the glycine zwitterion is less stable compared to the neutral form by up to 2 kcal/mol at all levels of theory. This is in contradiction with experimental estimate[43] that the zwitterionic form is more stable by 7.67 kcal/mol in term of the free energy of hydration at 298 K. The single-point results for ΔH ($NT_{gas} \rightarrow ZT_{solv}$) are also 4–6 kcal/mol higher than the experimental value. However, when both neutral and zwitterionic forms were fully optimized in aqueous solution, good agreement with experiment was observed. In particular, optimizing the zwitterionic structure in the solvent reaction field lowers its hydration energy by 4–5 kcal/mol for different levels of theory. This correlates with the large solvent effect on the zwitterionic structure mentioned above. Small solvent effects on both the structure and hydration energy were observed for the neutral form. Consequently, the glycine zwitterion was found to be more stable by 2.6–4.0 kcal/mol, which is consistent with the experimental observation. Without fully optimizing the glycine structures, particularly for the zwitterionic form, we would have reached the wrong conclusion regarding the accuracy of the GCOSMO solvation model. However, our calculated difference in free energies of hydration, ΔG ($NT_{solv} \rightarrow ZT_{solv}$), is too small by 3–4 kcal/mol compared to the experimental estimate.[43] Note that since neutral glycine does not exist in aqueous solution or in the solid state, direct measurement of ΔG ($NT_{solv} \rightarrow ZT_{solv}$) cannot be done. Thus, the difference between our result and experimental estimate can be due to the combination of errors in the GCOSMO model as well as in the thermodynamic cycle procedure for estimating this quantity from other experimental energetic values.[43] Even more encouraging result is that our calculated ΔH ($NT_{gas} \rightarrow ZT_{solv}$) is within the experimental uncertainly for all levels of theory considered here.

B. Efficiency and accuracy of the GCOSMO energy derivatives

In our previous study,[9] we have found that the GCOSMO solvation model costs on the average of 10%

TABLE III. Geometrical parameters (bond distances are in Å and angles in deg) of glycine zwitterion (C_s symmetry) in gas phase and aqueous solution.

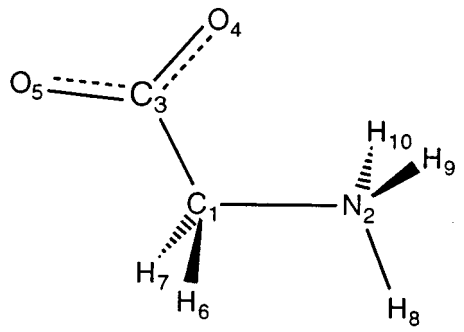

Coordinates	HG(g)	HF(solv)	MP2(solv)	B3LYP(solv)	BH&HLYP(solv)	Expt[a]
C_1–N_2	1.506	1.477	1.485	1.492	1.476	1.476
C_1–C_3	1.570	1.532	1.543	1.544	1.527	1.526
C_3–O_4	1.235	1.235	1.265	1.258	1.244	1.251
C_3–O_5	1.208	1.233	1.260	1.253	1.241	1.250
C_1–H_6	1.080	1.080	1.087	1.091	1.083	
N_2–H_8	1.005	1.006	1.018	1.021	1.012	
N_2–H_9	1.008	1.006	1.018	1.021	1.012	
N_2–C_1–C_3	105.9	111.3	110.7	110.9	111.2	111.9
O_4–C_3–C_1	111.6	117.4	116.8	116.6	116.8	117.5
O_5–C_3–C_1	114.1	115.1	115.2	114.8	114.9	117.1
H_6–C_1–N_2	108.3	108.2	108.0	107.8	107.9	
H_8–N_2–C_1	115.3	112.8	113.0	111.8	111.5	
H_9–N_2–C_1	107.3	111.1	110.6	111.2	111.5	

[a]Crystal structure is taken from Ref. 44.

more cpu time than the gas-phase calculation. Its analytical energy first derivatives are slightly more expensive and generally cost between 10%–40% extra cpu time per one Berny optimization step (one energy and one gradient calculation per step) compared to the gas-phase calculation. In particular, the percent extra cpu time is about 40% for the HF, 25% for the nonlocal DFT, and 10% for the MP2 level. Due to the cavity surface discretization, the GCOSMO energy gradient is not as accurate as in the gas-phase case. We can get geometry optimization converging with the maximum gradient of 0.002 a.u. and energy tolerance of 10^{-6} a.u. Since the cavity surface is generated at every optimization step, the convergence of the geometry optimization for solvated system is slightly slower, particularly when small changes in the geometry of the solute create new or delete surface elements from the previous step. Increasing the number of surface elements per atomic sphere and including the derivatives of the surface element areas, dispersion, repulsion, and cavity formation terms would improve the convergence and accuracy. Analytical second energy derivatives are now being implemented in our lab. Their applications for studying transition state structures and mechanisms of chemical reactions in solutions as well as IR spectra of solvated systems will be presented in a future study.

TABLE IV. Free energies of hydration and relative free energies (kcal/mol) of glycine (NT for neutral form) and its zwitterion (ZT) in aqueous solution.

	HF	MP2	B3LYP	BH&HLYP	Expt
Gas-phase geometries					
ΔG_{solv} (NT)	−14.17	−11.49	−11.42	−12.59	
ΔG_{solv} (ZT)	−45.69	−39.36	−38.03	−41.36	
ΔG ($NT_{solv}\rightarrow ZT_{solv}$)	2.16	0.02	1.19	1.54	−7.67[c]
ΔH ($NT_{gas}\rightarrow ZT_{solv}$)[a]	−15.02	−14.47	−13.23	−14.05	−19.2±1[b]
Optimized in solution					
ΔG_{solv}(NT)	−14.35	−11.65	−11.59	−12.73	
ΔG_{solv}(ZT)	−50.65	−43.56	−42.47	−45.99	
ΔG ($NT_{solv}\rightarrow ZT_{solv}$)	−2.63	−4.02	−3.09	−2.95	−7.67[c]
ΔH ($NT_{gas}\rightarrow ZT_{solv}$)[a]	−19.98	−18.67	−17.67	−18.68	−19.2±1[b]

[a]Entropy contribution at 298 K estimated to be 3 kcal/mol (from Ref. 41) was used in all calculated results.
[b]Taken from Ref. 42.
[c]Estimation taken from Ref. 43.

IV. CONCLUSION

We have presented explicit expressions for the first and second derivatives of the electrostatic solvation energy with respect to the solute nuclear coordinates for our recently proposed dielectric continuum solvation theory called generalized conductorlike screening model (GCOSMO). These derivatives have simple forms and can be incorporated into classical, quantum mechanical molecular orbital and density functional theories. Within the *ab initio* MO and DFT frameworks, these derivatives involve simple one-electron integrals for which efficient computational procedures are available in most *ab initio* MO computer program packages. Thus, additional computational cost is minimal. In fact, for the gradients, we found that they cost on the average of 40% extra cpu time per one Berny structure optimization step compared to the gas-phase calculations at the HF level, 25% at the nonlocal DFT, and 10% at the MP2 level of theory.

We have applied the GCOSMO analytical energy gradient to study hydration effects on structure and relative stability of glycine neutral and zwitterionic conformations at the HF, MP2, B3LYP, and BH&HLYP levels of theory using the 6-31G(d,p) basis set. By fully optimizing geometries of both the neutral and zwitterionic forms of glycine in aqueous solution, we found that solvent has small effect on the structure and hydration energy of the neutral form but has significant effect on the zwitterionic form. The optimized zwitterionic structures agree very well with the experimental crystal structure at all levels of theory considered here. Furthermore, the calculated enthalpy change for transfering glycine from the gas phase to aqueous solution, ΔH ($NT_{gas} \rightarrow ZT_{solv}$), is also in excellent agreement with available experimental data. The single point approach, which has been employed in many previous studies, where the gas-phase geometries were used for calculating hydration energies, yields significant errors. In particular, it predicts the neutral form to be more stable than the zwitterionic form in aqueous environment, that is in contradiction with experimental observation. This approach also yields 5–6 kcal/mol errors in the calculated ΔH ($NT_{gas} \rightarrow ZT_{solv}$).

The present study further confirms the accuracy and efficiency of the GCOSMO solvation model. Its simple analytical derivatives presented here open up new possibilities for studying solvent effects on conformations, exploring features on free energy surfaces of chemical reactions in solutions, and predicting spectroscopic properties of solvated systems. However, it is important to keep in mind that we have introduced several approximations such as neglecting the nonelectrostatic contribution to the total derivative in the present implementation of the GCOSMO derivatives. Such approximations were found to be small for the system considered here. However, further testing on the accuracy of the GCOSMO model on different systems is certainly needed and is being considered in our lab.

Note added in proof: The hydration energy of glycine zwitterion was first calculated to be -47 kcal/mol by using the surface constrained soft sphere dipoles model [A. Warshel, J. Phys. Chem. **83**, 1640 (1979)]. This, in fact, is in good agreement with our present results.

ACKNOWLEDGMENTS

This work is supported in part from the University of Utah and the National Science Foundation through a Young Investigator Award to T.N.T. We also thank Dr. Warshel for bringing to our attention the reference discussed in the added note above.

[1] J. Tomasi and M. Persico, Chem. Rev. **94**, 2027 (1994).
[2] C. J. Cramer and D. G. Truhlar, in *Reviews in Computational Chemistry*, edited by K. B. Lipkowitz and D. B. Boyd (VCH, New York, 1994), Vol. 6, p. 1.
[3] S. Miertuš, E. Scrocco, and J. Tomasi, Chem. Phys. **55**, 117 (1981).
[4] J. Tomasi, R. Bonaccorsi, R. Cammi, and F. J. Olivares del Valle, J. Mol. Struct. (Theochem) **80**, 401 (1991).
[5] A. Fortunelli and J. Tomasi, Chem. Phys. Lett. **231**, 34 (1994).
[6] J. L. Chen, L. Noodleman, D. A. Case, and D. Bashford, J. Phys. Chem. **98**, 11 059 (1994).
[7] A. A. Rashin, M. A. Bukatin, J. Andzelm, and A. T. Hagler, Biophys. Chem. **51**, 375 (1994).
[8] D. J. Tannor, B. Marten, R. Murphy, R. A. Friesner, D. Sitkoff, A. Nicholls, M. Ringnalda, W. A. Goddard, and B. Honig, J. Am. Chem. Soc. **116**, 11 875 (1994).
[9] T. N. Truong and E. V. Stefanovich, Chem. Phys. Lett. **240**, 253 (1995).
[10] E. V. Stefanovich and T. N. Truong, J. Comp. Chem. (submitted).
[11] T. N. Truong and E. V. Stefanovich, J. Phys. Chem. (submitted).
[12] R. Cammi and J. Tomasi, J. Chem. Phys. **101**, 3888 (1994).
[13] R. Cammi and J. Tomasi, J. Chem. Phys. **100**, 7495 (1994).
[14] M. K. Gilson, M. E. Davis, B. A. Luty, and J. A. McCammon, J. Phys. Chem. **97**, 3591 (1993).
[15] R. Bonaccorsi, R. Cammi, and J. Tomasi, J. Comp. Chem. **12**, 301 (1991).
[16] A. Klamt and G. Schüürmann, J. Chem. Soc. Perkin Trans. **II**, 799 (1993).
[17] E. L. Coitiño, J. Tomasi, and R. Cammi, J. Comp. Chem. **16**, 20 (1995).
[18] A. Pullman and B. Pullman, Q. Rev. Biophys. **7**, 505 (1975).
[19] K. Morokuma, J. Am. Chem. Soc. **104**, 3732 (1982).
[20] J. Aqvist and A. Warshel, Chem. Rev. **93**, 2523 (1993).
[21] J. J. Field, P. A. Bash, and M. Karplus, J. Comp. Chem. **11**, 700 (1990).
[22] J. L. Gao and X. F. Xia, Science **258**, 631 (1992).
[23] U. C. Singh and P. A. Kollman, J. Comp. Chem. **7**, 718 (1986).
[24] R. V. Staton, D. S. Hartsough, and J. Merz, J. Phys. Chem. **97**, 11 868 (1993).
[25] T. Wesolowski and A. Warshel, J. Phys. Chem. **98**, 5183 (1994).
[26] G. Alagona, C. Ghio, and P. A. Kollman, J. Mol. Struct. (Theochem) **166**, 385 (1988).
[27] J. S. Alper, H. Dothe, and D. F. Coker, Chem. Phys. **153**, 51 (1991).
[28] J. S. Alper, H. Dothe, and M. A. Lowe, Chem. Phys. **161**, 199 (1992).
[29] Y. Ding and K. Krogh-Jespersen, Chem. Phys. Lett. **199**, 261 (1992).
[30] R. F. Frey, J. Coffin, S. Q. Newton, M. Ramek, V. K. W. Cheng, F. A. Momany, and L. Schäfer, J. Am. Chem. Soc. **114**, 5369 (1992).
[31] C.-H. Hu, M. Shen, and F. H. Schaefer III, J. Am. Chem. Soc. **115**, 2923 (1993).
[32] J. H. Jensen and M. S. Gordon, J. Am. Chem. Soc. **113**, 3917 (1991).
[33] O. Kikuchi, T. Natsui, and T. Kozaki, J. Mol. Struct. (Theochem) **207**, 103 (1990).
[34] M. Mezei, P. K. Mehrotra, and D. L. Beveridge, J. Biomol. Struct. Dyn. **2**, 1 (1984).
[35] H. S. Rzepa and M. Yi, J. Chem. Soc. Perkin Trans. **2**, 531 (1991).
[36] L. R. Wight and R. F. Borkman, J. Am. Chem. Soc. **102**, 6207 (1980).
[37] D. Yu, D. A. Amstrong, and A. Rauk, Can. J. Chem. **70**, 1762 (1992).
[38] R. Bonaccorsi, P. Palla, and J. Tomasi, J. Am. Chem. Soc. **106**, 1945 (1984).
[39] A. G. Császár, J. Am. Chem. Soc. **114**, 9568 (1992).
[40] F. Jensen, J. Am. Chem. Soc. **114**, 9533 (1992).
[41] R. Bonaccorsi, F. Floris, P. Palla, and J. Tomasi, Thermochim. Acta **162**, 213 (1990).
[42] J. S. Gaffney, R. C. Pierce, and L. Friedman, J. Am. Chem. Soc. **99**, 4293 (1977).
[43] P. Haberfield, J. Chem. Educ. **57**, 346 (1980).
[44] P.-G. Jönsson and Å. Kvick, Acta Crystallorg., Sec. B **28**, 1822 (1972).
[45] H. Hoshi, R. Chûjô, Y. Inoue, and M. Sakurai, J. Chem. Phys. **87**, 1107 (1987).
[46] H. Hoshi, R. Chûjô, Y. Inoue, and M. Sakurai, J. Mol. Struct. (Theochem) **49**, 267 (1988).

[47] T. Furuki, A. Umeda, M. Sakurai, Y. Inoue, R. Chûjô, and K. Harata, J. Comp. Chem. **15**, 90 (1994).
[48] F. J. Olivares del Valle and J. Tomasi, Chem. Phys. **150**, 139 (1991).
[49] F. J. Olivares del Valle, M. A. Aguilar, and S. Tolosa, J. Mol. Struct. (Theochem) **98**, 223 (1993).
[50] F. J. Olivares del Valle and M. A. Aguilar, J. Comp. Chem. **13**, 115 (1992).
[51] F. J. Olivares del Valle, R. Bonaccorsi, R. Cammi, and J. Tomasi, J. Mol. Struct. (Theochem) **76**, 295 (1991).
[52] M. A. Aguilar, F. J. Olivares del Valle, and J. Tomasi, Chem. Phys. **150**, 151 (1991).
[53] J. A. Pople, R. Krishnan, H. B. Schlegel, and J. S. Binkley, Int. J. Quantum Chem. **S13**, 225 (1979).
[54] F. M. Richards, Annu. Rev. Biophys. Bioeng. **6**, 151 (1977).
[55] M. J. Frisch, G. W. Trucks, H. B. Schlegel, P. M. W. Gill, B. G. Johnson, M. W. Wong, J. B. Foresman, M. A. Robb, M. Head-Gordon, E. S. Replogle, R. Gomperts, J. L. Andres, K. Raghavachari, J. S. Binkley, C. Gonzalez, R. L. Martin, D. J. Fox, D. J. Defrees, J. Baker, J. J. P. Stewart, and J. A. Pople, GAUSSIAN 92/DFT, Revision G.3, Gaussian, Inc., Pittsburgh, Pennsylvania, 1993.
[56] E. V. Stefanovich and T. N. Truong, Chem. Phys. Lett. (submitted).
[57] F. M. Floris, J. Tomasi, and J. L. P. Ahuir, J. Comp. Chem. **12**, 784 (1991).
[58] W. L. Jorgensen and J. Tirado-Rives, J. Am. Chem. Soc. **110**, 1657 (1988).
[59] R. A. Pierotti, Chem. Rev. **76**, 717 (1976).
[60] A. D. Becke, J. Chem. Phys. **98**, 5648 (1993).
[61] A. D. Becke, J. Chem. Phys. **98**, 1372 (1993).
[62] C. Lee, W. Yang, and R. G. Parr, Phys. Rev. B **37**, 785 (1988).
[63] P. D. Godfrey and R. D. Brown, J. Am. Chem. Soc. **117**, 2019 (1995).
[64] K. Iijima, K. Tanaka, and S. Onuma, J. Mol. Struct. **246**, 257 (1991).
[65] B. G. Johnson, P. M. W. Gill, and J. A. Pople, J. Chem. Phys. **98**, 5612 (1993).
[66] P. M. W. Gill, B. G. Johnson, J. A. Pople, and M. J. Frisch, Int. J. Quantum Chem. **S26**, 319 (1992).